

Manuscript Number: NIMA-D-18-01280

Title: Pulse shape discrimination of CLYC scintillator coupled with a large SiPM array

Article Type: Full length article

Section/Category: Neutron Physics and Detectors

Keywords: neutron, scintillator, pulse shaping methods, SiPM, simulation, efficiency.

Corresponding Author: Miss Nesrine DINAR,

Corresponding Author's Institution: CERN

First Author: Nesrine DINAR

Order of Authors: Nesrine DINAR; Damiano Celeste; Marco Silari; Alberto Fazzi

Abstract: This paper discusses measurements performed to evaluate the possibility to build a neutron probe based on a CLYC scintillator coupled with a large SiPM array. The use of a large SiPM array allows optimising the light collection, necessary for spectrometry. However, a large SiPM array leads to huge capacitance, whose main impact is to slow down the input signals. Therefore, pulse shape discrimination (PSD) is lost due to the electronic process. To solve this problem, an electronic board was designed to extract the fastest scintillation decay times from the crystal without cutting the crystal response. The impact of using a large SiPM array instead of a PMT is evaluated by comparing the PSDs and the scintillation decay times. A figure of merit (FOM) of 2.3 was found with the SiPM versus a value of 2.64 for the PMT. In addition, the neutron efficiency was measured and compared to the one simulated with the MCNP code. The angular dependence and the linearity range in dose rate were also evaluated.



**European Organisation for Nuclear Research**  
**Organisation européenne pour la recherche nucléaire**

Nesrine Dinar  
CERN  
Route de Meyrin  
CH-1211 Geneva 23  
+41 22 766 24 32  
+41 75 411 62 58  
nesrine.dinar@cern.ch

Editorial board  
Nuclear Instruments & Methods in Physics Research

Geneva, 4 December 2018

Dear Editors,

Please find enclosed the manuscript: "PULSE SHAPE DISCRIMINATION OF CLYC SCINTILLATOR COUPLED WITH A LARGE SIPM ARRAY" by Nesrine Dinar, Damiano Celeste, Marco Silari, Alberto Fazzi and Vincenzo Varoli for your consideration for publication in Nuclear Instruments & Methods in Physics Research (section A).

All authors contributed significantly to the submitted work and approved to the revisions made in the manuscript. The results of this research have not yet been published elsewhere and we hope that you will find our manuscript suitable for publication in Nuclear Instruments & Methods in Physics Research (section A). We would like to publish the manuscript with colour figures in the online version, and with black and white figures in the paper version.

The manuscript describes original work and is not under consideration by any other journal. We appreciate your time and look forward to your response.

Yours sincerely,

Nesrine Dinar

# Pulse shape discrimination of CLYC scintillator coupled with a large SiPM array

N. Dinar<sup>1,2,\*</sup>, D. Celeste<sup>2</sup>, M. Silari<sup>2</sup>, A. Fazzi<sup>3</sup>, V. Varoli<sup>3</sup>

<sup>1</sup>LAL, Univ.Paris-Sud, CNRS/IN2P3, Universite Paris-Saclay, Orsay, France

<sup>2</sup>CERN, 1211 Geneva 23, Switzerland

<sup>3</sup>Politecnico of Milano, Via La Masa 34, 20156 Milano, Italy

1        ***Abstract***—This paper discusses measurements performed to evaluate the possibility to build a neutron probe based on a  
2        CLYC scintillator coupled with a large SiPM array. The use of a large SiPM array allows optimising the light collection,  
3        necessary for spectrometry. However, a large SiPM array leads to huge capacitance, whose main impact is to slow down the  
4        input signals. Therefore, pulse shape discrimination (PSD) is lost due to the electronic process. To solve this problem, an  
5        electronic board was designed to extract the fastest scintillation decay times from the crystal without cutting the crystal  
6        response. The impact of using a large SiPM array instead of a PMT is evaluated by comparing the PSDs and the scintillation  
7        decay times. A figure of merit (FOM) of 2.3 was found with the SiPM versus a value of 2.64 for the PMT. In addition, the  
8        neutron efficiency was measured and compared to the one simulated with the MCNP code. The angular dependence and the  
9        linearity range in dose rate were also evaluated.

10        ***Keywords***—neutron, scintillator, pulse shaping methods, SiPM, simulation, efficiency.

## 11        1. INTRODUCTION

12        Radiation detectors with dual neutron/ $\gamma$ -ray sensitivity and robust discrimination features are in great demand nowadays  
13        to reduce the size and the complexity of conventional systems, generally provided with two different detectors for  
14        independent measurements. The advent of the CLYC scintillator material has drawn the attention of the scientific  
15        community due to its excellent energy resolution, sensitivity to both neutrons and  $\gamma$ -rays and pulse shape discrimination  
16        (PSD) features. CLYC has a density of 3.31 g/cm<sup>3</sup> and a peak-emission wavelength around 373 nm, which well matches  
17        the response of many commercially available photomultipliers (PMTs). In the framework of the B-RAD project, the  
18        development of a radiation survey meter capable of operating in the presence of a strong magnetic field [1], we started  
19        the development of a portable neutron probe based on a CLYC coupled with a SiPM array. The choice of SiPMs is  
20        justified by crucial requirements: the insensitivity to external magnetic fields and the low operating voltage with respect

21 to PMTs. The gain is similar to a PMT. The small size allows building an extremely compact, light and robust  
22 mechanical device. The PSD performance and decay times of the CLYC are evaluated with the SiPM and compared to  
23 those obtained with a PMT. The measured and simulated efficiencies are also compared. The linearity in dose rate as  
24 well as the angular response of the CLYC are evaluated.

## 25 2. EXPERIMENTAL DETAILS

### 26 2.1. Material

27 A cylindrical CLYC crystal 25.4 mm in diameter and 25.4 mm thick from Radiation Monitoring Devices [2] and a SiPM  
28 array J-30035-64P-PCB from SensL [3] were used. A CLYC crystal with the lithium element enriched in  ${}^7\text{Li}$  at >99% is  
29 used in this work. This enrichment suppresses the sensitivity to thermal neutrons allowing a better detection of fast  
30 neutrons through the  ${}^{35}\text{Cl}(n,p){}^{35}\text{S}$  and  ${}^{35}\text{Cl}(n,\alpha){}^{32}\text{P}$  reactions. The Q values of these reactions are 615 keV and 937 keV,  
31 respectively. The energy deposition of the products linearly depends on the energy of the incident neutron. Thus neutron  
32 spectrometry without resorting to an unfolding code is in principle possible up to 8-10 MeV. Above this energy, multiple  
33 reaction channels and excited states result in a spread out of the response function [4]. Since the CLYC is hygroscopic, a  
34 cylindrical housing protects it from moisture. The SiPM array is made up of sixty-four  $3\times 3\text{ mm}^2$  silicon elements, each  
35 consisting of 5676 APD-cells (Avalanche Photo Diodes of  $35\times 35\text{ }\mu\text{m}^2$  size). The whole size of the array well matches 1-  
36 inch cylindrical scintillators. The response of the CLYC+SiPM was compared with that obtained with a PMT R6231-100  
37 from HAMAMATSU [5].

38

39 Taking into account the SiPM standard output, the slow response of the electronics prevents distinguishing the initial  
40 differences in the shapes of the n/ $\gamma$  signals from the CLYC. To achieve this goal, we had to increase the speed of the  
41 signal by trying to extract the fastest scintillation times from the crystal without cutting its response. The method  
42 consisted in compensating the slow component of the signal by exploiting the pole-zero cancellation method. An RC  
43 circuit is implemented in series, after the amplification stage, to compensate for the pole due to the high capacitance of  
44 the photo-detector and to introduce a new pole at higher frequency. Following this idea, a first prototype of the circuit  
45 was built (Figure 1).

46

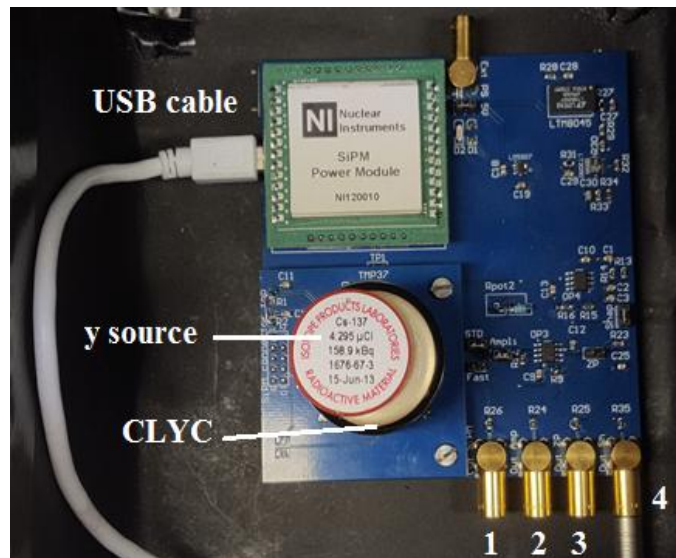


Fig. 1 Prototype of the neutron probe

47

48

## 49 2.2. PSD

50 A  $^{252}\text{Cf}$  source was used to study the  $n/\gamma$  discrimination. About 100,000 signals were recorded and analyzed off-line. The  
 51 first step for the PSD analysis was to align all the waveforms to a common zero. However, unlike in the case of the PMT  
 52 signal output, the Savitzky–Golay low pass filter was applied to increase the signal-to-noise ratio without distorting the  
 53 signal. Several algorithms for PSD exist, in this work the charge integration method was employed [6]. The principle of  
 54 charge comparison is to integrate two parts of each pulse: the charge of the entire pulse ( $Q_{\text{total}}$ ) and the charge in the tail  
 55 ( $Q_{\text{tail}}$ ). The difference in the ratio of the  $Q_{\text{tail}}$  to the  $Q_{\text{total}}$  (the  $Q_{\text{ratio}}$ ) is calculated and used to discern which type of  
 56 radiation generated the pulse.

57

58 A figure of merit (FOM) is used to establish the ability to discriminate between pulses generated by photons and  
 59 neutrons. The FOM is calculated from the histogram of the  $Q_{\text{ratio}}$  versus peak height data assuming that the pulse  
 60 distributions are Gaussian. The FOM is calculated after a PSD has been performed, measuring the width and locations of  
 61 the peaks in the histogram of the pulse shape data. The choice of the two timing intervals, at which the integration of the  
 62 pulse should be measured, is based upon a series of measurement that optimize the discrimination.

## 63 2.3. Neutron efficiency

64 To estimate the neutron detection efficiency, the scintillator was irradiated with AmBe source neutrons in the calibration  
 65 laboratory (CALLAB) of the Radiation Protection group at CERN [7]. The activity of the source was 100 GBq emitting  
 66  $6.4 \times 10^6$  neutrons/s. The intrinsic efficiency was defined as the ratio between the neutron fluence detected by the CLYC

67 and the neutron fluence incident on the crystal. The CLYC was placed at 135 cm distance from the source. The data  
68 acquisition was set to approximately 1h30 to obtain the maximum number of files that can be registered by the Lecroy  
69 HDO6104 oscilloscope (100,000) and analysed off-line. The measured efficiency was compared to the one simulated  
70 with the Monte Carlo N-Particle 6 (MCNP6) code developed by Los Alamos National Laboratory [8], to obtain a  
71 theoretical estimate of the efficiency of CLYC to fast neutrons. In the input file, surface, cell and data cards were defined.  
72 A 1 inch right cylinder made of CLYC enriched with 99%  $^7\text{Li}$ , 75%  $^{35}\text{Cl}$  and 25%  $^{37}\text{Cl}$  was simulated. The evaluated  
73 nuclear data file ENDF/B-VII.0 was implemented for these calculations [9]. The scintillator was placed in a concrete  
74 room of  $13 \times 13 \times 13 \text{ m}^3$  volume that modelled the CALLAB geometry [10]. The neutron energy spectrum was generated  
75 according to the AmBe energy binning defined in the ISO-8529-2 norm [11]. The energy spectrum of the emitted  
76 neutrons is a continuum up to around 10 MeV. The source definition was a point source. The number of source particles  
77 used in the simulation was  $10^7$ , sufficient to achieve low statistical uncertainty while minimizing the computing time.

78 Neutron interactions within CLYC-7 result in the production of protons, alpha particles and deuterons [12]. The tallying  
79 of these products enables evaluating the neutron interactions. The F8 Pulse Height Tally, which records the energy  
80 deposited in a cell by each source particle and its secondary particles, was used. The F8 tally was associated to pulse  
81 height light (PHL) treatment in order to model the pulse height energy spectrum of the CLYC detector [8]. The PHL tally  
82 treatment allows for the conversion of the energy deposition (F6 tally) into detector pulse height (F8 tally).

83 The intrinsic efficiency was calculated as the ratio between the total number of particles created inside the CLYC  
84 (protons, alpha particles and deuterons) and the number of neutrons impinging on the CLYC surface.

#### 85 *2.4. Scintillation decay times*

86 The neutron and photon signals were averaged and normalized to their peak amplitude according to the highest FOM, to  
87 produce the so-called standard pulse. The standard pulses contribute to eliminate noise fluctuations in individual signals  
88 and reveal the details on the prompt and delayed shape. To study the decay time under photon and neutron irradiations,  
89 the standard pulses were fitted with exponential decay curves, each decay time constant corresponding to a specific  
90 scintillation mechanism [13]. For  $\text{Ce}^{3+}$  doped crystals, up to four mechanisms contribute to the scintillation  
91 corresponding to four different energy transfers, which occur at different timescales:

92  
93 - Direct e-/hole capture by  $\text{Ce}^{3+}$  ( $\text{Ce}^{3+}$ ): after absorbing a  $\gamma$ -ray, free electrons and holes are created in the conduction  
94 band and valence band, respectively. These free electrons and holes may be trapped by a  $\text{Ce}^{3+}$  ion and the observed decay

95 time is characteristic of the lifetime of the excited state of  $Ce^{3+}$ . This type of fast energy transfer is desired for impurity  
96  $Ce^{3+}$  activated inorganic scintillator materials.

97

98 - Binary e-/hole recombination ( $V_k$ ): instead of being captured by the  $Ce^{3+}$  ion, the hole produced initially in the valence  
99 band is unstable and will create a molecular complex called  $V_k$  center.

100

101 - Self-trapped exciton (STE) diffusion/emission: if the  $V_k$  centre is captured by an electron from the conduction band,  
102 before being trapped by a  $Ce^{3+}$  ion, a STE is formed. STE is luminescent itself and has a lifetime of several  
103 microseconds.

104

105 - Core-to-valence luminescence (CVL): in case of chloro elpasolite (such as the CLYC), a fourth mechanism may occur.  
106 When the incident high-energy photon excites an electron from the upper core band into the conduction band, the  
107 resulting hole is short lived and will recombine with an electron from the valence band. If the process is radiative, it is  
108 called CVL. CVL is characterized by a short decay time (0.6 to 3 ns).

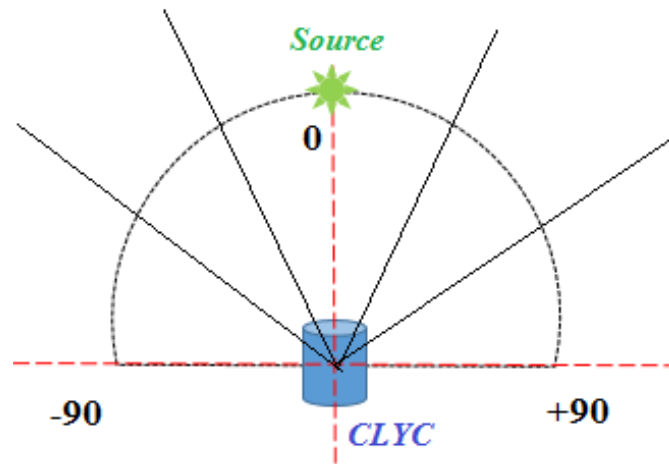
#### 109 *2.5. Linearity in dose rate*

110 The count rate linearity of a CLYC + photodetector system is determined by its time resolution, which is defined as the  
111 minimum time between successive scintillation pulses that the detection system can distinguish. This time interval may  
112 be limited by the decay time of the scintillator, the frequency characteristics of the signal processing circuit, and the  
113 timing characteristics of the photodetector's electronics. The decay time of the scintillation pulses from CLYC detectors  
114 is as long as a few microseconds, resulting in significant pulse pile-up at moderate input count rates.

115 To study the linearity range of CLYC and the effect of SiPM (instead of traditional PMT) on this range, measurements  
116 were performed with  $\gamma$ -sources. The main component of the output signals are from  $\gamma$ -interactions with the crystal, the  
117 neutron efficiency being <1%. Therefore, the saturation will occur with  $\gamma$ -signals. The discriminator threshold affects the  
118 linearity range. Thus, in order to compare the linearity range of the CLYC when coupled with the SiPM or PMT, the  
119 same discriminator threshold (330 keV) was fixed through an energy calibration measurement. Several waveforms from  
120  $^{137}Cs$  and  $^{60}Co$  sources were registered with the oscilloscope. Data were then manipulated via software (Python script) in  
121 order to obtain source spectra. Four  $^{137}Cs$  sources of different activities were used (300 MBq, 3 GBq, 30 GBq and  
122 300 GBq). The dose rate was changed by modifying the distance to the source and the activity of the source.

123 2.6. Angular dependence

124 The energy states of molecules consist of a series of discrete levels, which affect the scintillation mechanism in inorganic  
125 materials. Therefore, the mechanism is dependent on the crystal lattice, which means that the response of the scintillator  
126 can be anisotropic. To study the angular response of the detector, the CLYC was coupled with the PMT and irradiated in  
127 a pure  $\gamma$  ( $^{137}\text{Cs}$ ) and a mixed  $\gamma$ /neutron (AmBe) field. The system CLYC + PMT was placed at different angles from  $-90^\circ$   
128 to  $+90^\circ$  at interval of  $30^\circ$  (see Figure 2).



129

130 Fig. 2 Schematic of the irradiation set-up for determining the angular response of the CLYC.

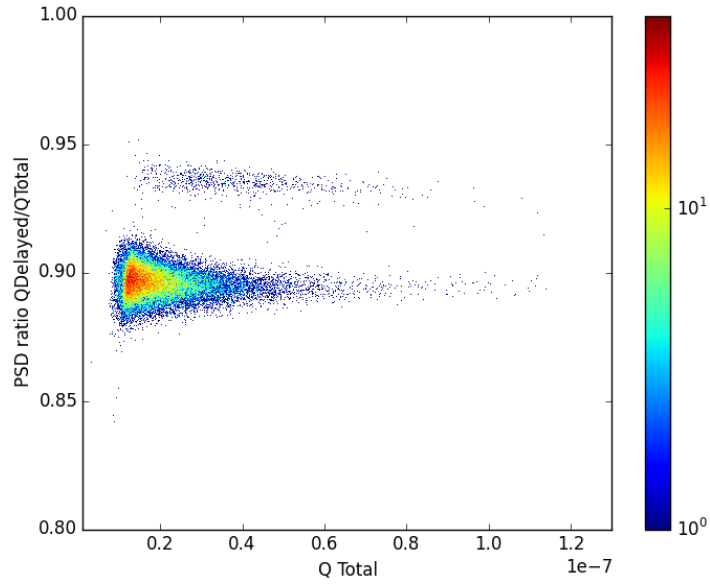
131 3. RESULTS AND DISCUSSION

132 3.1. PSD

133 With a cut at the Q value of the neutron reaction (615 keV) the best FOM are 2.97 (PMT) and 2.30 (SiPM). Figure 3  
134 shows the two-dimensional PSD plot obtained with the CLYC coupled with the SiPM and the specific board (see Figure  
135 1). Two populations are clearly visible, the upper one corresponding to neutrons. The  $^{252}\text{Cf}$  neutron spectrum is extracted  
136 by integrating the neutron signals and it is shown in Figure 4. For a qualitative comparison, Figure 5 shows the  $^{252}\text{Cf}$   
137 reference neutron spectrum of ISO8529-1. The first approximation of the measured neutron energy distribution is  
138 coherent.

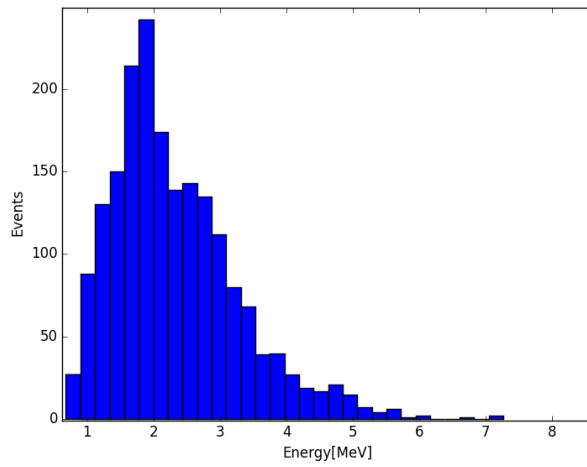
139





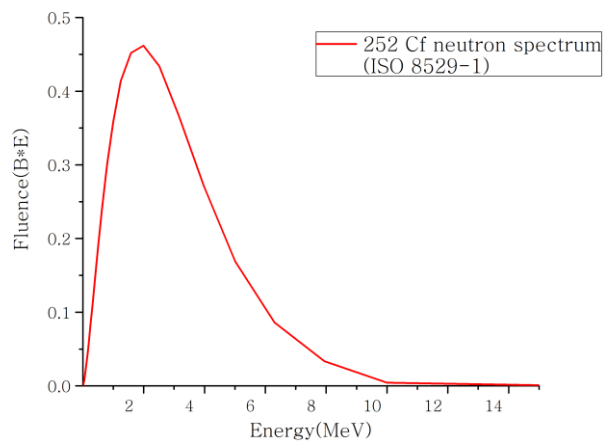
140

141 Fig. 3 2D PSD plot with  $\gamma$  (lower) and neutron (upper) populations.



142

143 Fig. 4  $^{252}\text{Cf}$  neutron spectrum from CLYC coupled with the SiPM array J-30035-64P-PCB.



144

145 Fig. 5  $^{252}\text{Cf}$  reference neutron spectrum from ISO 8529-1.

146 3.2. Neutron efficiency

147 The optimal time window to optimize the FOM was applied (90 ns - 1  $\mu$ s) and only the neutron Gaussian peak was  
 148 integrated from the projection of the PSD ratio on the x-axis. The neutron intrinsic efficiency was found to be 0.8% for  
 149 an AmBe source. To obtain a calibration factor the fluence was folded with the fluence to dose conversion factor [11].  
 150 An experimental calibration factor of 12 nSv/count was found. This value is in excellent agreement with both the  
 151 simulated efficiency (0.7% equivalent to a calibration factor of 11 nSv/count) and with literature data ([14] and [15]  
 152 giving 0.7% and 0.8%, respectively).

153 3.3. Scintillation decay times

154 Table 1 presents the results of the fitting procedure. For the PMT, the gamma waveform reveals four decay times: 2 ns  
 155 (T1), 48 ns (T2), 637 ns (T3) and 4.8  $\mu$ s (T4). Considering the two exponential decay fits, the neutron waveform at room  
 156 temperature presents a component with 598 ns (T3) and 4493 ns (T4). Correlating these results with the literature, these  
 157 mechanisms may be attributed to T1=CVL, T2=Ce<sup>3+</sup>, T3=V<sub>k</sub>, T4=STE+Ce<sup>3+</sup> [13].

158

159 To study the influence of the photodetector response on the CLYC decay times, the CLYC was coupled with the SiPM.  
 160 As with the PMT two decay times were found for the neutron waveform (517 ns and 4.2  $\mu$ s). These times are comparable  
 161 to the PMT (598 ns and 4.4  $\mu$ s) and can be attributed to the same mechanism. However only three decay times were  
 162 found for the  $\gamma$ -pulse. The T1 component of the signal due to CVL is absent. Moreover the T2 component is slower with  
 163 the SiPM than with the PMT (131 ns against 48 ns). The slow recovery time of the SiPM is responsible for the  
 164 disappearance of T1 and the decrease of T2 of the measured waveforms. This result shows that only the fast component  
 165 of the signal (hundred ns) is slowed down by the SiPM response.

166

167 Table 1. Measured decay times for  $\gamma$  and neutron induced reactions on CLYC at room temperature.

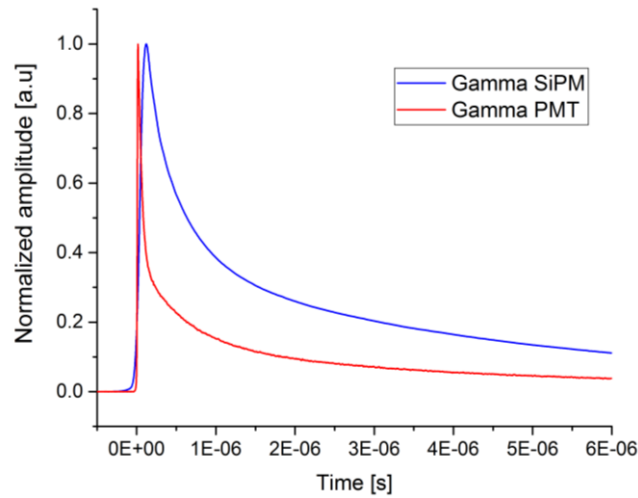
		<b>T1</b>	<b>T2</b>	<b>T3</b>	<b>T4</b>
		(ns)	(ns)	(ns)	(ns)
<b>PMT</b>	$\gamma$	2	48	637	4821
	Neutron	-	-	598	4493
<b>SIPM</b>	$\gamma$	-	131	494	4215
	Neutron	-	-	517	4208

168

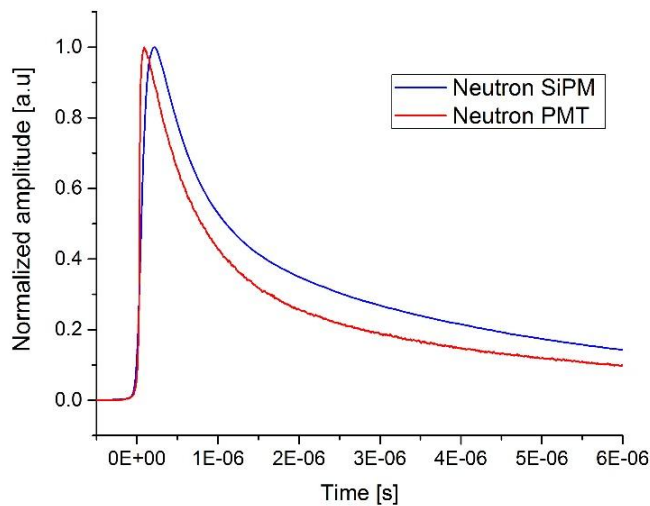
169 Figure 6 shows the photon and neutron standard pulses measured with the PMT and the SiPM. The neutron waveforms  
 170 are quite similar but the absence of CVL is clear on the photon signal obtained with the SiPM. The difficulty to

171 discriminate the  $\gamma$  and neutron signals when the CLYC is coupled with the SiPM was reported by several authors (see for  
172 example ref. [16]). However, although the fast components are affected by the SiPM and consequently are responsible  
173 for the reduction in the PSD capability as compared to a PMT, the PSD is still possible with an excellent FOM of 2.3.

174



175



176

177 Fig. 6 Neutron and  $\gamma$  signals with PMT (red) and SiPM (blue).

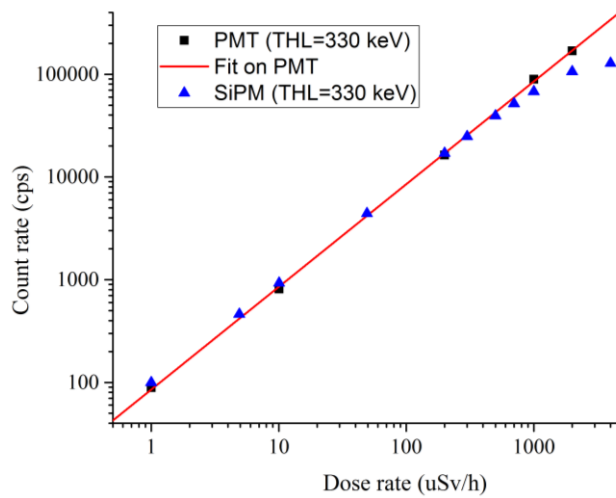
### 178 3.4. Linearity in dose rate

179 Figure 7 shows the count rate as a function of dose rate for both the PMT and SiPM at the same threshold. For clarity,  
180 only the fit to the PMT data points is shown. The saturation appears at about 1 mSv/h for the SiPM while the PMT is still  
181 linear. This discrepancy may be explained by the difference in the timing of the signals. As seen in Figure 6, the  $\gamma$  signals  
182 with the PMT are faster than the ones obtained with the SiPM. The larger the signal width the higher the probability of  
183 pile up effects, thus the range of linearity of the detector is shortened.

184 3.5. Angular response

185 Figures 8 and 9 show the angular response of the CLYC when irradiated with  $^{137}\text{Cs}$  and AmBe sources, respectively. The  
186 first effect seen is that the response of the CLYC is symmetric around its  $0^\circ$  axis. For example the count rates at  $-30^\circ$  and  
187  $+30^\circ$  are very similar. Another effect is that the count rate increases with angle (up to 17%), the minimum being at  $0^\circ$ .  
188 This effect can be attributed to the smaller solid angle provided by the cylindrical geometry of the sensitive volume when  
189 viewed head-on. Indeed the difference of solid angle when irradiating the CLYC head on as compared with irradiating it  
190 side on is about 20%.

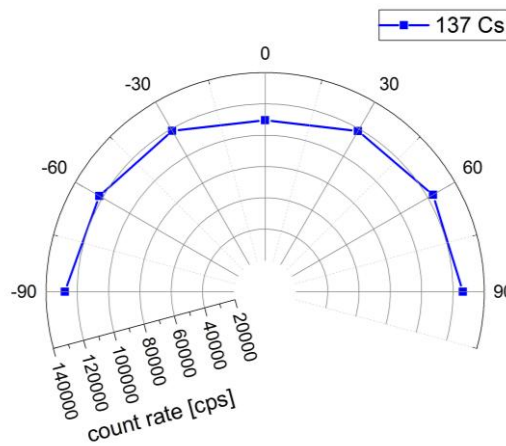
191



192

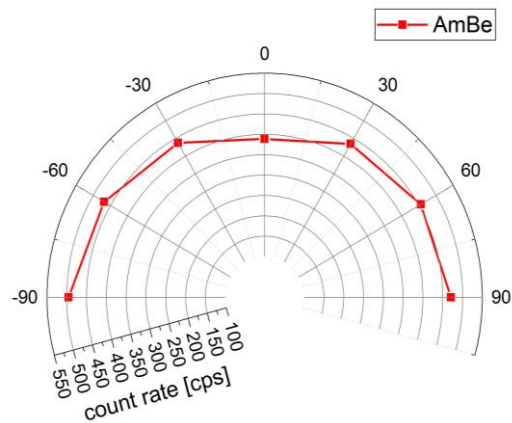
193 Fig. 7 Count rate as a function of dose rate obtained with the SiPM (blue) and PMT (black) at the energy threshold of 330 keV. The red line represents  
194 the linear fit to the PMT data.

195



196

197 Fig. 8 Directional response of the CLYC to a  $^{137}\text{Cs}$  source.



198

199 Fig. 9 Directional response of the CLYC to an AmBe source.

200

#### 201 4. CONCLUSIONS

202 A CLYC scintillator was investigated for its potential use in fast neutron detection/spectrometry. The CLYC was coupled  
 203 to a SiPM as well as a PMT and the results were compared.

204

205 The capacity of the CLYC+SiPM to discriminate  $\gamma$  and neutron signals was the more challenging part when dealing with  
 206 such a large array, since the total capacitance increases with the number of pixels. The extraction of the fastest  
 207 scintillation decay time constants from the crystal and the shortening of the falling time of the signal without cutting the  
 208 crystal response was achieved through the development of specific electronics. An excellent FOM of 2.3 was found  
 209 approaching the result obtained with PMT. Shortening the signals allows increasing the linearity range and the frequency  
 210 of the events at which the CLYC is sensitive.

211

212 The system CLYC+SiPM is linear in dose rate up to 1 mSv/h where it starts showing a slight saturation effect. The  
 213 angulation response was measured with both  $\gamma$  and neutron sources. A variation of 20% in count rate was found between  
 214 front and lateral irradiation ( $0^\circ$  and  $90^\circ$ ).

215

216 Finally, the fast neutron efficiency was simulated with MCNP and the results were validated experimentally. Similar  
 217 efficiency values of approximately 0.8% were found (i.e about 0.2 counts per second for a dose rate of 1 uSv/h). The  
 218 CLYC could be used as a stationary detector to monitor both  $\gamma$  and neutron dose rates in workplaces. Another potential  
 219 application for the CLYC is its use for homeland security (non-proliferation, border security) to improve the detection of  
 220 special nuclear materials (SNM). Spontaneous and induced fission events in SNM produce neutrons and  $\gamma$ -rays, which

221 can be detected and well separated thanks to the excellent discrimination capabilities of the CLYC. The fission products  
222 have an energy between 500 keV and 10 MeV that fit the measuring range of the CLYC. CLYC neutron detectors can  
223 therefore be used as dual mode to detect  $\gamma$ -ray and neutron in SNM search and monitoring applications.

224

225

## 226 5. REFERENCES

227

- 228 [1] Celeste, D. Curioni, A. Fazzi, A. Perrin, Silari, M. Varoli, V. B-Rad: a radiation survey meter for operation in intense magnetic field,  
229 submitted to JINST.
- 230 [2] <http://rmdinc.com/clyc/>
- 231 [3] <http://SensL.com/downloads/ds/DS-MicroJseries.pdf>
- 232 [4] N.D Olympia, P. Chowdhury, E.G Jackson and C.J Lister, Fast neutron response of  $^6\text{Li}$  depleted CLYC detectors up to 20 MeV, Nucl. Instrum.  
233 Meth. A. 433 441 (2014)
- 234 [5] <https://www.hamamatsu.com/jp/en/product/type/R6231/>
- 235 [6] A.P. Siddavatam, Method of pulse shape discrimination, International Journal of Application or Innovation in Engineering, special issue of  
236 International technological conference, (2014)
- 237 [7] F. Pozzi, R. Garcia Alia, M. Brugger, P. Carbonez, S. Danzeca, B. Gkotse, M.R. Jaekel, F. Ravotti, M. Silari and M. Tali, CERN irradiation  
238 facilities, Radiation Protection Dosimetry 180, 120-124 (2017)
- 239 [8] D.B. Pelowitz, MCNP6 User's Manual", Version 1.0. Los Alamos National Laboratory Report, LA-CP-11-00634, 2013.
- 240 [9] M.B Chadwick and al., ENDF/B-VII.0: Next generation evaluated nuclear data library for nuclear science and technology, nuclear data sheets,  
241 vol.107, pp.2931-3060 (2006).
- 242 [10] <http://irradiation-facilities.web.cern.ch/>
- 243 [11] ISO International Standards. ISO 8529-1 Reference Neutron Radiations – Part 1: Characteristics and Methods of Production (2001).
- 244 [12] R.S.Woolf and al., Response of the Li-7 enriched CLYC-7 scintillator to 6-60 MeV neutrons Nucl. Instrum. Methods Phys. Res. A 803, 47–  
245 54(2015)
- 246 [13] E. V. D. van Loef, J. Glodo, W. M. Higgins, K. S. Shah, Optical and scintillation properties of  $\text{Cs}_2\text{LiYCl}_6:\text{Ce}^{3+}$  and  $\text{Cs}_2\text{LiYCl}_6:\text{Pr}^{3+}$  crystals, IEEE  
247 Transactions on Nuclear Science 52.
- 248 [14] A. Mentana et al, Measurement of fast neutron efficiency of  $^6\text{Li}$  and  $^7\text{Li}$  enriched CLYC scintillators, J. Phys.: Conf. Ser. 763 012006 (2016)
- 249 [15] A. Giaz and al., The CLYC-6 and CLYC-7 response to  $\gamma$ -rays, fast and thermal neutrons, Nucl. Instrum. Meth. A. 810 132 (2016).
- 250 [16] B. Budden, et al., Analysis of  $\text{Cs}_2\text{LiYCl}_6:\text{Ce}^{3+}$ (CLYC) waveforms as read out by solid state photomultipliers, IEEE Nuclear Science Symposium  
251 Conference Rec., N1-164, pp. 347–350, (2012).
- 252